

Filtering Power Divider/Combiner Using Substrate Integrated Waveguide (SIW)-Based 180° Hybrid

A.-R. Moznebi¹ and K. Afrooz^{2*}

Received:2016-02-29

Accepted:2016-09-08

Abstract

This paper presents a filtering power divider (PD)/power combiner (PC) using substrate integrated waveguide (SIW)-based 180° hybrid. The utilized 180° hybrid includes a standard H-plane 3-dB coupler and a broadband 90° phase shifter. The phase shifter is composed of non-radiating longitudinal slots patterned on the top conducting surface of the SIW. We have added the filtering property to the structure by an array of dissimilar transverse slots. The slots dimensions are obtained by the extracted external quality factor, coupling coefficient and the relationship between them and the slots dimensions. The proposed structure is designed for 8.2 GHz and investigated by ADS simulator. The results show the fractional bandwidth of the sum and difference ports are 13.7% and 14.93%, respectively. For sum operation, the minimum insertion loss is 3.78 dB and the return loss is above 25 dB in the passband. For difference operation, the minimum insertion loss is 3.81 dB and the return loss is above 26 dB in the passband.

Keywords: 180° hybrid, phase shifter, power combiner, power divider, substrate integrated waveguide (SIW).

1. Introduction

Power dividers (PDs) are of elementary passive structures in the design and realization of various microwave components including phase shifters, power amplifiers, antenna arrays, and mixers [1].

Waveguide PDs have the benefits of the low loss, high Q-factor, and high power capacity [2]. In [3], a PD has been investigated by this structure. This circuit has the disadvantages of the

high cost, bulky volume, and difficult integration with planar circuits.

Substrate integrated waveguide (SIW) is a new structure of waveguide which is realized by two parallel rows of via holes in a metalized planar substrate [4]. Nowadays, this structure is attracting much attention because of its low cost, low loss, and easy integration with planar circuits. It is inferred from the scientific reports concerning SIW-based PDs that achieving high levels of isolations between the output ports of a PD is not an easy task [5,6].

The Wilkinson PD [7] has been widely used in microwave systems because of the good bandwidth, high isolation, good return loss, and low insertion loss. In this circuit, the isolation resistor between the output ports is not grounded, which is difficult for heat dissipation. Moreover, in high frequency applications, the variation in the results may be introduced by the coupling between the output ports. Therefore, the Wilkinson PD is suitable for low power applications. In [8], a half mode substrate integrated waveguide (HMSIW) Wilkinson PD has been reported.

To tailor the frequency response of the PD in a specific frequency band, we can add a built-in bandpass filter to it. This will result in further integration, as well. Several PDs/power combiners (PCs) with the bandpass response are mentioned in the published papers [9-11]. In [9], a laminated waveguide magic-T with the embedded chebyshev filter response has been developed in a multilayer LTCC. In this design, the complex mechanism and multilayer are the disadvantages of the circuit. In [10], a single-layer PCB process can be realized. However, this design has comparatively large phase imbalance. A magic-T with bandpass filtering response based on SIW technology is reported in [11]. This design has comparatively large insertion loss. In addition, the main disadvantage in [9-11] is their narrow operating bands. Fig. 1 depicts the SIW PD linkage.

In this paper, a filtering PD/PC using SIW-based 180° hybrid is presented. The used 180° hybrid is organized by a standard H-plane 3-dB coupler and a broadband 90° phase shifter. This design has many advantages, such as low cost, low insertion loss, good return loss, good channels isolation, and compatibility with planar circuits.

¹ M.Sc. Student, Department of Electrical Engineering, Shahid Bahonar University of Kerman, Kerman, Iran.
moznebi@eng.uk.ac.ir

² Assistant Professor, Department of Electrical Engineering, Shahid Bahonar University of Kerman, Kerman, Iran.
afrooz@uk.ac.ir

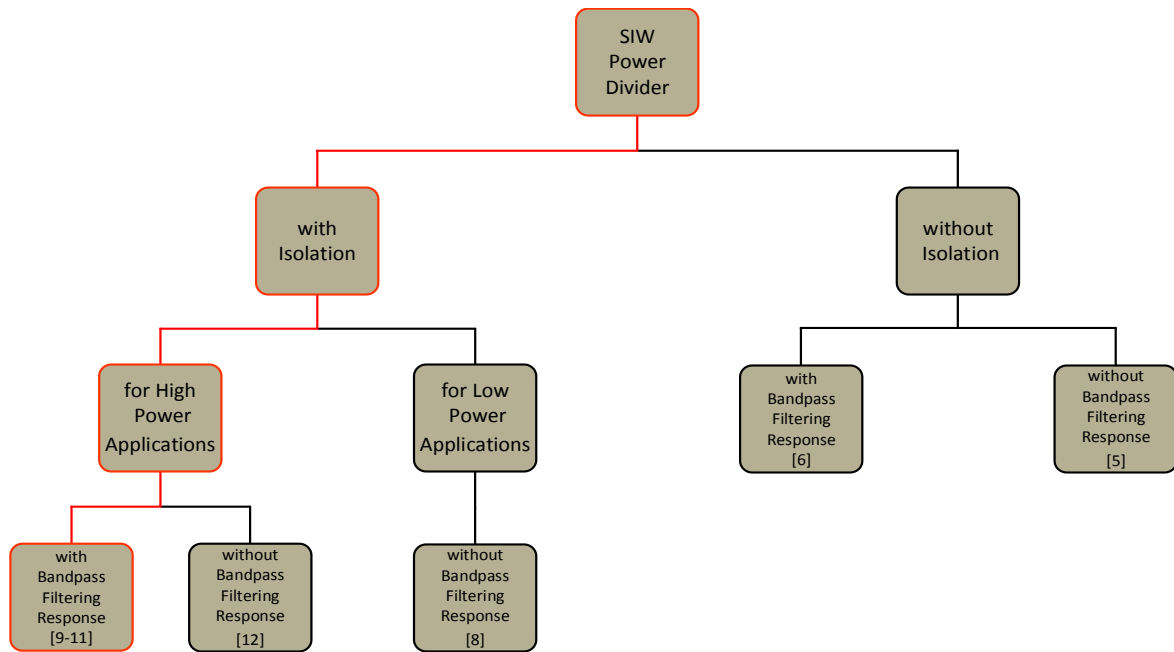


Figure 1: SIW PD linkage.

2. Design Procedure

A. SIW design

Since the SIW is a quasi-rectangular waveguide, only TE_{n0} modes can propagate and the TE_{10} mode is the dominant mode. In this structure, the TM modes cannot be guided due to the dielectric gaps created by via separations [13]. In an SIW structure the radiation loss can be minimized if [14]:

$$\frac{s}{d} \leq 2 \quad (1)$$

where d refers to the diameter of the vias and s is their longitudinal spacing. The cutoff frequency of the SIW can be determined by the following formulae [15]:

$$f_{c(TE_{10})} = \frac{c}{2W_{eff} \sqrt{\mu_r \epsilon_r}} \quad (2)$$

In (2), c is the velocity of light in the free space, ϵ_r is the relative permittivity of the substrate, μ_r is the relative permeability of the substrate, and W_{eff} refers to the equivalent width of the SIW, which can be calculated by [16]:

$$W_{eff} = W - 1.08 \cdot \frac{d^2}{s} + 0.1 \cdot \frac{d^2}{W} \quad (3)$$

In (3), W displays the transverse spacing of the two vias that are located at both sides of the SIW.

B. SIW-to-microstrip transition design

In the input, a microstrip-to-SIW transition is used [17]. As shown in Fig. 2, this transition is composed of a tapered microstrip section and two matching vias. The specified parameters are [17]:

$$L_{t1} = 0.2368 \lambda_{gMS} \quad (4)$$

$$W_{t1} = W_m + 0.1547W \quad (5)$$

$$s_1 = 0.6561s_2 \quad (6)$$

$$W_3 = 0.8556W \quad (7)$$

λ_{gMS} is the guided wavelength of the microstrip line calculated at the center frequency [17]:

$$\lambda_{gMS} = \frac{\lambda_{g0}}{\sqrt{\epsilon_{reff}}} \quad (8)$$

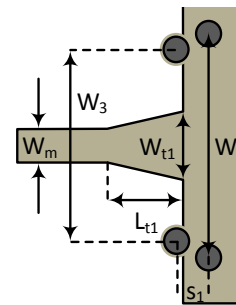


Figure 2: Geometry of the SIW-to-microstrip transition.

where ϵ_{reff} refers to the effective dielectric constant of the microstrip line and λ_{g0} refers to the wavelength in free space.

C. Filter design

To design the filtering function, the adjusted transverse slots are added to the circuit [18].

Each part of the SIW between two transverse slots is considered as a resonator. Here, two resonators are embedded by etching three rectangular slots on the top layer of each patch. The coupled resonators play the role of the bandpass filter. The geometry and equivalent circuit of the SIW filter are shown in Fig. 3.

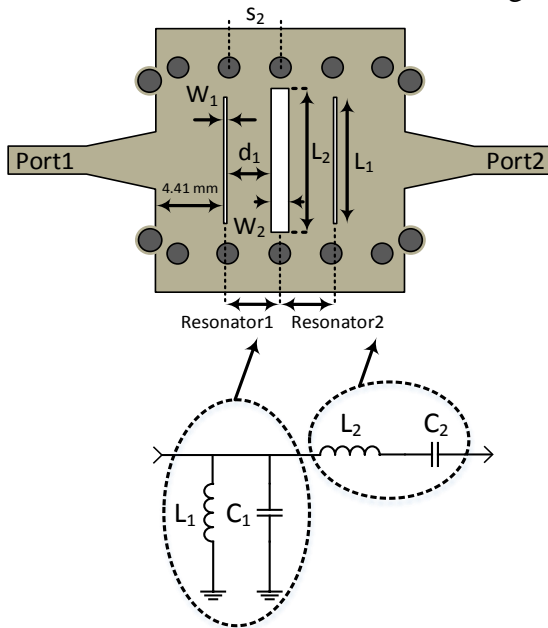
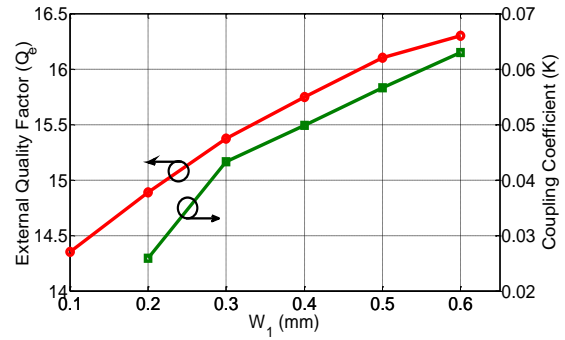
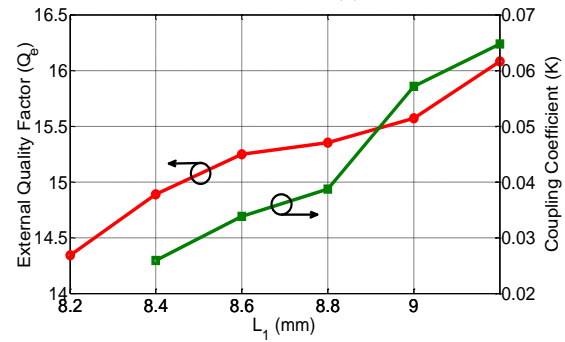


Figure 3: Geometry and equivalent circuit of the SIW filter.

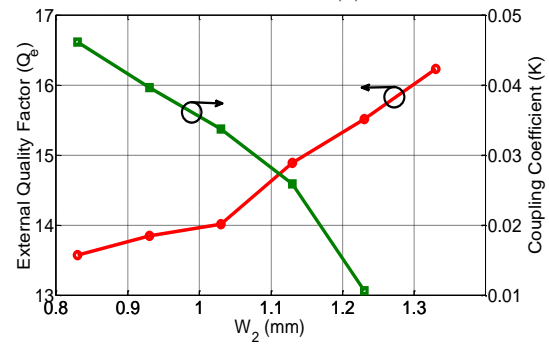
The desired external quality factor and the coupling coefficient are of determinative parameters in the design of the rectangular slots. Before that, according to the filter requirements, the design parameters (coupling coefficient and external quality factor) can be defined by the circuit elements of a low-pass prototype filter [19]. In this design, the considered external quality factor and coupling coefficient are 15 and 0.025, respectively. The width and length of the rectangular slots are varied in the ADS environment to determine the relationship between the physical dimensions and external quality factor and coupling coefficient. The external quality factor and coupling coefficient can be evaluated by using the following relations [19]:



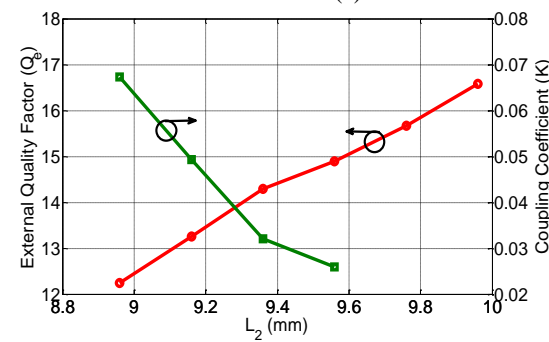
(a)



(b)



(c)



(d)

Figure 4: External quality factor and coupling coefficient as a function of: (a) W_1 (b) L_1 (c) W_2 (d) L_2 .

$$Q_e = \frac{2f_0}{\text{BW}} \quad (9)$$

$$K = \frac{f_1^2 - f_2^2}{f_1^2 + f_2^2} \quad (10)$$

where f_0 refers to the resonance frequency, BW refers to the 3 dB bandwidth, and f_1 and f_2 represent the higher and lower resonant frequencies of the coupled resonators. Fig. 4

shows the width and length of the rectangular slots versus the external quality factor and coupling coefficient between the two resonators.

D. Filtering SIW PD/PC design

In the first step, an 180° hybrid is designed by a standard H-plane 3-dB coupler and a broadband 90° phase shifter. Figs. 5 and 6 show the configurations of the 180° hybrid and proposed filtering SIW PD/PC. In the H-plane 3-dB coupler, the initial value of the W_c can be obtained as that of the rectangular waveguide narrow-wall coupler of the same coupling ratio in the same frequency band. This parameter can be optimized in a full-wave simulation.

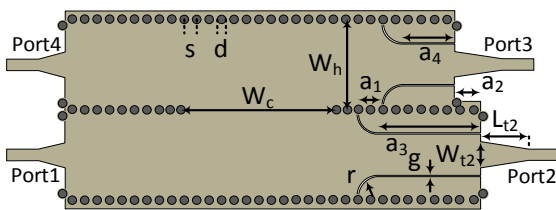


Figure 5: Configuration of the 180° hybrid.

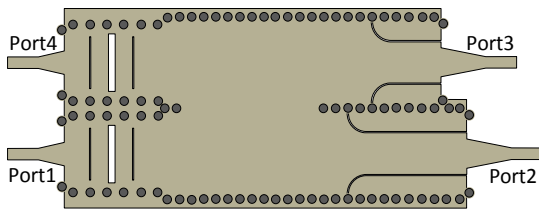


Figure 6: Configuration of the filtering SIW PD/PC.

In the broadband 90° phase shifter, which is presented in [20], the parameters can be evaluated after working through some mathematical manipulation. The scattering parameters of the 180° hybrid are illustrated in Fig. 7. These results clearly show the circuit has the best performance in 8~8.5 GHz frequency band.

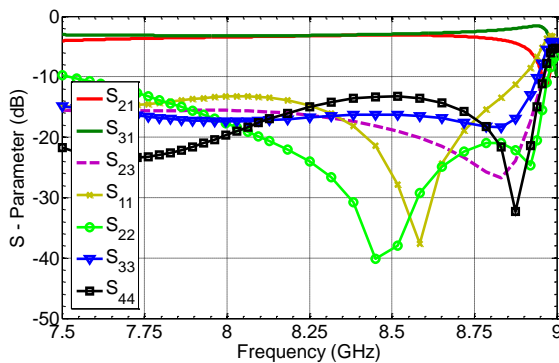


Figure 7: S-parameters of the 180° hybrid.

Table I illustrates the dimensions of the filtering SIW PD/PC. In this Table, the parameters of $s, s_2, d, W,$ and W_h can be achieved from Equations

(1)-(3), the parameters of $W_{t1}, L_{t1}, W_3,$ and s_1 can be calculated from Equations (4)-(7), the parameters of $W_1, L_1, W_2,$ and L_2 can be determined from Fig. 4, and the parameters of $a_1, a_2, a_3, a_4, r,$ and g can be calculated by [20]. On the other hand, the parameters of $W_{t2}, L_{t2}, W_c,$ and d_1 can be obtained by optimization. Also, W_m is width of a 50 Ω microstrip line.

Table I
Dimensions of the proposed structure (units:mm)

W	12.36	L_{t2}	7.36
W_1	0.2	a_1	3.97
W_2	1.13	a_2	4.22
W_3	10.57	a_3	16.39
W_c	24.13	a_4	8.19
W_h	14.77	s	1.98
W_m	1.86	s_1	1.83
W_{t1}	3.77	s_2	2.79
W_{t2}	4.7	d	1.45
L_1	8.4	d_1	2.9
L_2	9.54	r	3.17
L_{t1}	4.24	g	0.2

It should be noted here that the width of the SIW filter is less than the 180° hybrid. Since, the best performance of the 180° hybrid is above the cutoff frequency of the dominant mode.

3. Results

Based on above design results, the proposed filtering PD/PC using SIW-based 180° hybrid is simulated on a single layer Rogers RO4003C substrate with a dielectric constant of 3.55, thickness of 0.8128 mm, and loss tangent of 0.0027. Also, in simulation process, the dielectric and conductive losses are considered.

The simulated results are shown in Figs. 8-10. For sum operation, the 3 dB bandwidth is 1.119 GHz ranging from 7.607 to 8.726 GHz (13.7%). Moreover, the minimum insertion loss is 3.78 dB and the return loss is above 25 dB in the passband. For difference operation, the 3 dB bandwidth is 1.226 GHz ranging from 7.595 to 8.821 GHz (14.93%). Moreover, the minimum insertion loss is 3.81 dB and the return loss is above 26 dB in the passband. In this circuit, the return loss is above 17.5 dB in port 2 and 19 dB

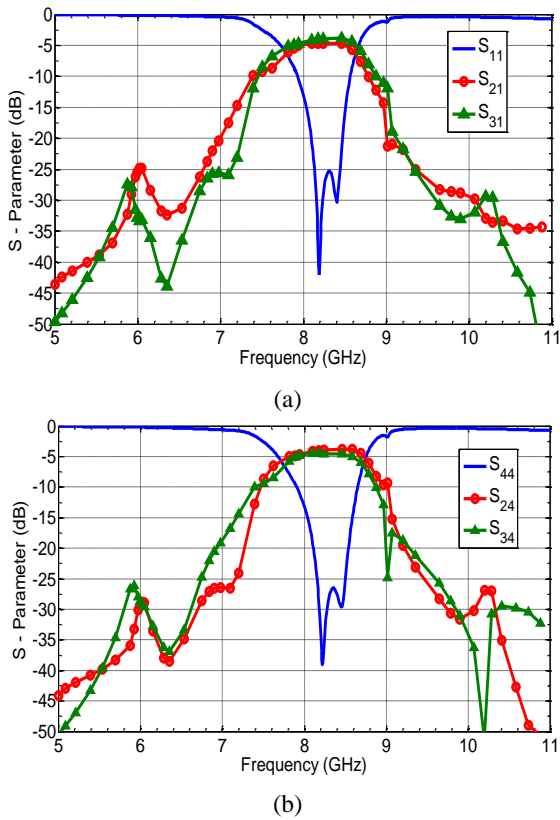


Figure 8: S-parameters of the proposed structure with a frequency axis range of 5 to 11 GHz (a) S_{11} , S_{21} , and S_{31} (b) S_{44} , S_{24} , and S_{34} .

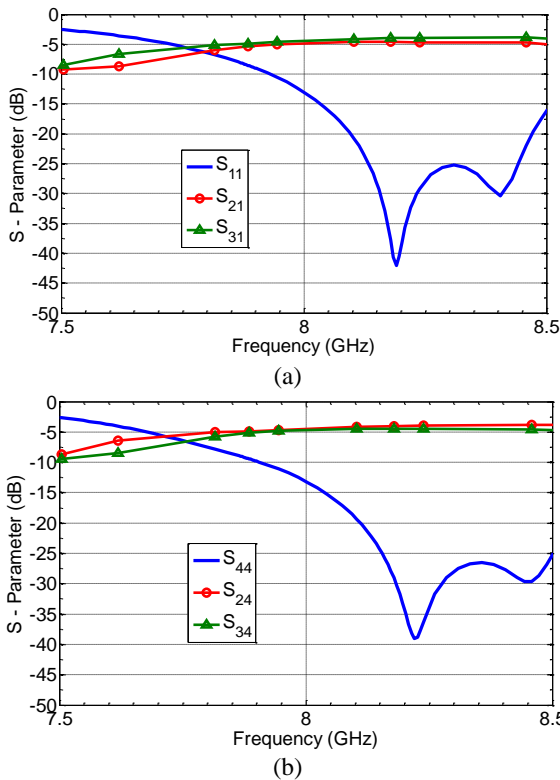


Figure 9: S-parameters of the proposed structure with a frequency axis range of 7.5 to 8.5 GHz (a) S_{11} , S_{21} , and S_{31} (b) S_{44} , S_{24} , and S_{34} .

in port 3 and the isolation is better than 34 dB between output ports and 20 dB between sum and difference ports.

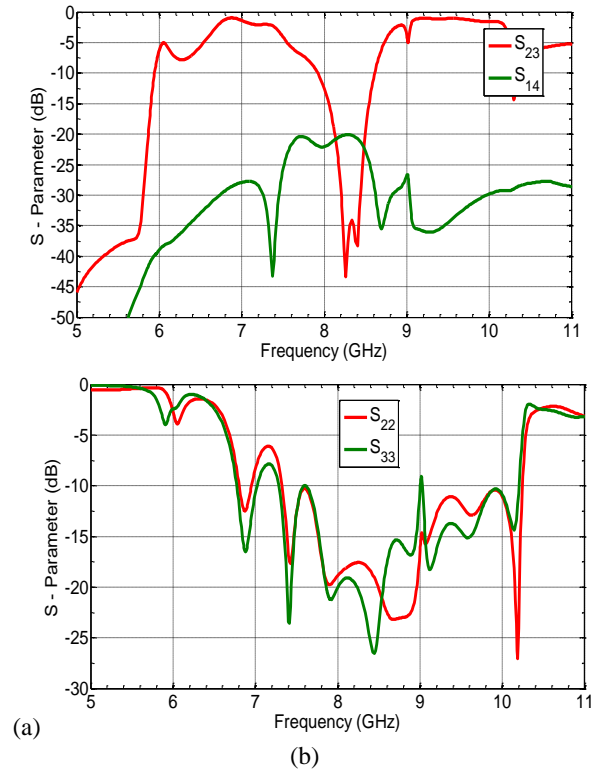


Figure 10: S-parameters of the proposed structure (a) S_{23} and S_{14} (b) S_{22} and S_{33} .

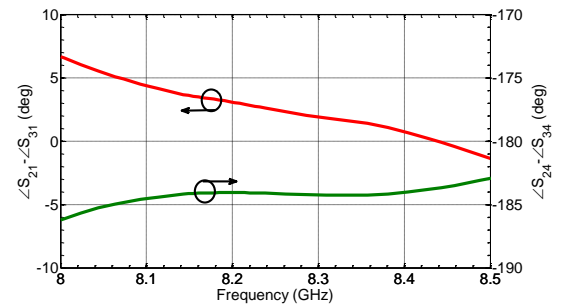


Figure 11: Phase imbalance results of the proposed structure.

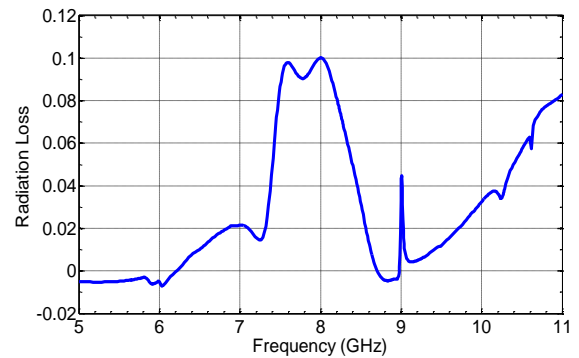


Figure 12: Radiation loss of the proposed structure.

Fig. 11 indicates the phase imbalance in the passband of the proposed structure which is less than 6.5° for sum operation and 6° for difference operation. In Fig. 12, the radiation loss (R_r) is less than 0.1 under the conditions of lossless metal and substrate. This parameter guarantees the

produced radiation is negligible. The radiation loss is defined as:

$$R_r = 1 - S_{11}S_{11}^* - S_{21}S_{21}^* - S_{31}S_{31}^* - S_{41}S_{41}^* \quad (11)$$

In Table II, a comparison between the simulated results of the proposed structure and measured results of [9-11] is summarized.

Table II
Comparison with other works

Ref.	Size ($\lambda_g^2 / \lambda_g^3$)	FBW (%)	IL (dB)	Results
[9]	$1.18 \times 1.26 \times 0.15$	6	2.24	Meas.
[10]	1.72×2.57	3.9	2	Meas.
[11]	2.67×2.67	0.77	1.913	Meas.
This work	1.66×4	14.93	0.811	Sim.

In this Table, the advantages in fractional bandwidth and insertion loss are very obvious. Furthermore, the size of the proposed structure is compact than [11] and its design process is much more simple than that of [9].

4. Conclusion

In this paper, a filtering PD/PC using SIW-based 180° hybrid has been proposed and investigated. The 180° hybrid has been realized by the standard H-plane 3-dB coupler and 90° broadband SIW phase shifter. To design the filtering function, two resonators have been embedded by etching three rectangular slots on the top layer of each patch. In this circuit, good performance such as low cost, efficient heat sinking, high power handle, and compatibility with planar circuits has been achieved. Compared with the previously reported circuits, this filtering SIW PD/PC can be widely used in microwave and millimeter-wave systems.

References

[1] Y. Wu, Y. Liu, Q. Xue, S. Li, and C. Yu, "Analytical design method of multiway dual-band planar power dividers with arbitrary power division", *IEEE Trans. Microw. Theory Tech.*, vol. 58, no. 12, pp. 3832-3841, November, 2010.
 [2] X. P. Chen, and K. Wu, "Substrate Integrated Waveguide Filter: Basic Design Rules and Fundamental Structure Features", *IEEE Microw.*

Magazine, vol. 15, no. 5, pp. 108- 116, July-August, 2014.
 [3] K. Song, Y. Fan, and B. Zhang, "Ku-band multiway rectangular waveguide power divider", *Microw. Optical Tech. Lett.*, vol. 52, no. 11, pp. 2560-2563, August, 2010.
 [4] H. Uchimura, T. Takenoshita, and M. Fujii, "Development of a "laminated waveguide"", *IEEE Trans. Microw. Theory Tech.*, vol. 46, no. 12, pp. 2438-2443, November, 1998.
 [5] X. Zou, C. M. Tong, and D. W. Yu, "Y-junction power divider based on substrate integrated waveguide", *Electron. Lett.*, vol. 47, no. 25, pp. 1375-1376, December, 2011.
 [6] S. Y. Chen, D. S. Zhang, and Y. T. Yu, "Wideband SIW power divider with improved out-of-band rejection", *Electron. Lett.*, vol. 49, no. 15, pp. 943-944, July, 2013.
 [7] E. J. Wilkinson, "An N-way hybrid power divider", *IRE Trans. Microw. Theory Tech.*, vol. 8, no. 1, pp. 116-118, January, 1960.
 [8] Z. Y. Zhang, and K. Wu, "Broadband half-mode substrate integrated waveguide (HMSIW) Wilkinson power divider", In *IEEE Microw. Symposium Digest*, Atlanta, GA, pp. 879-882, 2008.
 [9] T. M. Shen, T. Y. Huang, C. F. Chen, and R. B. Wu, "A laminated waveguide magic-T with bandpass filter response in multilayer LTCC", *IEEE Trans. Microw. Theory Tech.*, vol. 59, no. 3, pp. 584-592, February, 2011.
 [10] U. Rosenberg, M. Salehi, J. Bornemann, and E. Mehrshahi, "A novel frequency-selective power combiner/divider in single-layer substrate integrated waveguide technology", *IEEE Microw. Wirel. Compon. Lett.*, vol. 23, no. 8, pp. 406-408, June, 2013.
 [11] P. Li, H. Chu, and R. S. Chen, "SIW magic-T with bandpass response", *Electron. Lett.*, vol. 51, no. 14, pp. 1078-1080, July, 2015.
 [12] Z. Y. Zhang, Y. R. Wei, and K. Wu, "Broadband millimeter-wave single balanced mixer and its applications to substrate integrated wireless systems", *IEEE Trans. Microw. Theory Tech.*, vol. 60, no. 3, pp. 660-669, March, 2012.
 [13] J. E. Rayas-Sánchez, and V. Gutierrez-Ayala, "A general EM-based design procedure for single-layer substrate integrated waveguide interconnects with microstrip transitions", In *IEEE Microw. Symposium Digest*, Atlanta, GA, pp. 983-986, 2008.
 [14] K. Wu, D. Deslandes, and Y. Cassivi, "The substrate integrated circuits-a new concept for high-frequency electronics and optoelectronics", In *Telecommunications in Modern Satellite, Cable and Broadcasting Service*, pp. P-III, 2003.
 [15] Y. Cassivi, L. Perregrini, P. Arcioni, M. Bressan, K. Wu, and G. Conciauro, "Dispersion characteristics of substrate integrated rectangular waveguide", *IEEE*

Microw. Wirel. Compon. Lett., vol. 12, no. 9, pp. 333-335, September, 2002.

[16] F. Xu, and K. Wu, "Guided-wave and leakage characteristics of substrate integrated waveguide", IEEE Trans. Microw. Theory Tech., vol. 53, no. 1, pp. 66-73, January, 2005.

[17] Z. Kordiboroujeni, and J. Bornemann, "New Wideband Transition From Microstrip Line to Substrate Integrated Waveguide", IEEE Trans. Microw. Theory Tech., vol. 62, no. 12, pp. 2983-2989, November, 2014.

[18] S. W. Wong, K. Wang, Z. N. Chen, and Q. X. Chu, "Design of millimeter-wave bandpass filter using electric coupling of substrate integrated waveguide (SIW)", IEEE Microw. Wirel. Compon. Lett., vol. 24, no. 1, pp. 26-28, December, 2014.

[19] J. S. G. Hong, and M. J. Lancaster, Microstrip filters for RF/microwave applications. Wiley, 2004.

[20] Z. Y. Zhang, K. Wu, and Y. R. Wei, "Broadband delay compensation phase shifter using slotted substrate integrated waveguide structure", In IEEE Microw. Symposium Digest, Baltimore, MD, pp. 1-4, 2011.